Journal Pre-proofs

Magnetic stimulation of gold fiducial markers used in Image-Guided Radiation Therapy: evidences of hyperthermia effects

Paolo Arosio, Matteo Avolio, Marco Gargano, Francesco Orsini, Salvatore Gallo, Jacopo Melada, Letizia Bonizzoni, Nicola Ludwig, Ivan Veronese

PII: S0263-2241(19)31107-8
DOI: https://doi.org/10.1016/j.measurement.2019.107242
Reference: MEASUR 107242

To appear in: *Measurement*

Received Date: 18 February 2019
Revised Date: 24 September 2019
Accepted Date: 3 November 2019

Please cite this article as: P. Arosio, M. Avolio, M. Gargano, F. Orsini, S. Gallo, J. Melada, L. Bonizzoni, N. Ludwig, I. Veronese, Magnetic stimulation of gold fiducial markers used in Image-Guided Radiation Therapy: evidences of hyperthermia effects, *Measurement* (2019), doi: https://doi.org/10.1016/j.measurement.2019.107242

Magnetic stimulation of gold fiducial markers used in Image-Guided Radiation Therapy: evidences of hyperthermia effects

Paolo Arosio,[1,2,3], Matteo Avolio,[3,4,5], Marco Gargano[1], Francesco Orsini[1,2,3], Salvatore Gallo[1,2], Jacopo Melada[1], Letizia Bonizzoni[1], Nicola Ludwig[1,*], Ivan Veronese[1,2,3]

[1]Dipartimento di Fisica, Università degli Studi di Milano, Via Celoria 16, 20133 Milano (Italy)

[2]Istituto Nazionale di Fisica Nucleare, Sezione di Milano, Via Celoria 16, 20133 Milano (Italy)

[3]Consorzio Interuniversitario Nazionale per la Scienza e Tecnologia dei Materiali (Italy)

[4]Dipartimento di Fisica, Università degli Studi di Pavia, Via Bassi 6, 27100 Pavia (Italy)

[5]Istituto Nazionale di Fisica Nucleare, Sezione di Pavia, Via Bassi 6, 27100 Pavia (Italy)

Corresponding author:

**Nicola Ludwig*

Università degli Studi di Milano

via Giovanni Celoria 16 - 20133 Milano, Italy

e-mail: nicola.ludwig@unimi.it

Abstract

A promising approach in oncology consists in combining Radiation Therapy (RT) with Magnetic Fluid Hyperthermia (MFH). Modern day RT takes advantage by imaging techniques able to provide information about the correct patient set-up, target position and movement during the treatments. For these purposes, gold fiducial markers, implanted into the tumors, or in their proximity, are used in the so-called Image-Guided Radiation Therapy (IGRT).

In this study, hyperthermia produced by different gold fiducial markers under the application of an alternating magnetic field in the typical conditions used in Magnetic Fluid Hyperthermia (MFH) clinical trials was investigated. The temperature increase of different types of gold fiducial markers and of tissue mimicking hydrogel phantoms containing the fiducials were measured during the magnetic stimulation by means of a high-resolution thermal camera and a fiber optic temperature sensor.
The results demonstrated that, within few tens of seconds after the start of the magnetic stimulation, the gold fiducial markers might reach temperatures higher than 70°C. Local increases of the hydrogel temperature to values higher than 45°C were also measured. These evidences highlight the need to evaluate carefully the presence and location of gold fiducial markers in patients undergoing combined IGRT and MFH treatments in order to prevent any thermal ablation of health tissues surrounding the markers.

Keywords

Gold fiducial markers, Magnetic Fluid Hyperthermia, IGRT, Thermography, Hydrogel, eddy currents.

1. Introduction

Current treatment strategies for several oncological pathologies are based on the synergic combination of different techniques. Radiation therapy (RT) is one of the most widely used approach. Indeed, more than 14 million new cancer patients are diagnosed globally each year and approximately half of them can benefit from RT treatment at least once during the course of their disease [1].

Modern RT increasingly uses conformal delivery techniques, which require an accurate patient positioning and tumor targeting. This aspect is even more important in the case of irradiation of moving organs, e.g. organs influenced by breathing. The most used imaging techniques in the so-called Image Guided Radiation Therapy (IGRT) are those based on X-rays [2].

In such case, millimetric or sub-millimetric radiopaque metallic fiducial markers can be implanted into the lesions, or in their close proximity. These markers are easily visible by X-ray imaging and allow target localization and patient set up verification [3,4]. Gold markers are more commonly used, as they provide high levels of image contrast. It is worth noting that fiducial markers based on nanostructured gold particles are also being developed to be used in various diagnostic and therapeutic procedures requiring image-guided approaches [5-7].

Meanwhile, Magnetic Fluid Hyperthermia (MFH) in combination with RT is recently gaining importance in oncology [8]. In MFH technique, magnetic nanomaterials (normally iron oxides nanoparticles) directly implanted in the tumour mass at high doses (approximately 50 mg/cm^3), under the action of an externally applied alternating magnetic field (AMF), can generate a certain amount of local heat depending on the frequency f and the amplitude H of field. The success of MFH was recently demonstrated on glioblastoma multiform and prostate cancers in clinical trials, that certify a survival extension of patients had undergone the combined therapy [9,10]. At the same time, other types of hyperthermia that use different external stimuli (microwaves, laser, ultrasound, etc.) are implemented in clinical practice. For all these treatments, the reason to combine radiotherapy with hyperthermia is to increase the RT efficacy in cancer therapy strategies. In fact, hyperthermia could enhance blood flow and vascular permeability to tumor and could cause several biological processes more

pronounced in tumor cells, e.g. protein denaturation and damage to cytoskeleton, inducing ablation and eventually necrosis and apoptosis [8].

In particular, gold materials at nanoscale, properly functionalized and due to their intrinsic biocompatibility, are used in several therapeutic treatments as hyperthermic agents, and combined with RT [11-15]

In the case of MFH treatment, the first step consists in the removal of metallic materials within approximately 40 cm from the tumor to avoid heat up during the procedure. Typically, these materials include rather massive objectives like titanium clamps, metallic fillings in teeth, crowns and implants, shoulder joint replacements, cardiac pacemakers, and defibrillators [16]. In fact, it is well known that when a conducting material is simulated by an AMF, eddy currents are induced within the conductor with a consequent heat release due to Joule effect. Such phenomena could occur also in gold and it is exploited in many industrial applications, including melting processes, if appropriate frequencies and magnetic field intensities are chosen.

Aim of this study is to evaluate the level of heat that gold fiducial markers may release when stimulated by the application of an AMF in experimental conditions similar to those used in MFH clinical practice, i.e. frequency f = 109.8 kHz and AMF of 16.15 kA/m.

2. Materials and Methods

2.1 Gold fiducial markers

Three different types of gold fiducial markers (CIVCO Medical Solutions) were considered [17]:

(i) Bone Fiducial Marker: sphere, 2 mm in diameter, recommended for head and neck IGRT treatments;

(ii) Gold Soft Tissue Marker: cylinder, 3 mm long and 1.6 mm in diameter, with knurled surface to inhibit migration, specifically designed for IGRT at soft tissues as prostate, breast and abdomen;

(iii) PointCoil™ Fiducial Marker: helical coil, 5 mm long and 0.6 mm in diameter, recommended to minimize the artifacts in IGRT of prostate, lung and abdomen.

Images of the investigated samples are shown in Figure 1.

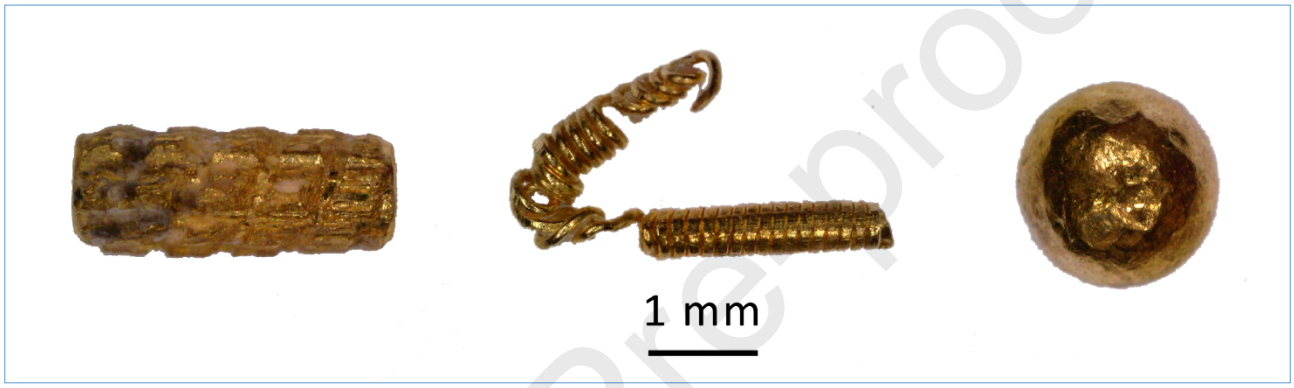

Figure 1. Images of the gold fiducial markers used in the study. The helical coil was partially unfolded in order to better show the dimensions of the gold wire.

Energy Dispersive X-Ray Fluorescence (ED-XRF) spectroscopy analyses were initially performed on the fiducial markers to check their elemental composition. The results confirmed the 99.9% of gold content, as certified by the vendor. Further details of the methods used for ED-XRF measurements are given in the supplementary material, together with examples of ED-XRF spectra (Figure. 1S).

Afterwards, one sphere and two cylinders were covered with glue and carbon black in order to modify the emissivity from the very low value of gold, less than 0.1, to the one as much as possible similar of a black body [18]. The effectiveness of the change in emissivity was verified by thermal reflectance measurements. The black cover enabled to measure, by means of a thermal camera, the heat produced by the fiducial markers individually placed over a suitable polystyrene support inserted into a homogenous magnetic field region (see section 2.3).

2.2 Phantoms

In order to model the heat transfer properties occurring into soft tissues surrounding the fiducial markers in case of MFH treatments, hydrogel phantoms based on poly(vinyl-alcohol) (PVA) cross-linked with glutaraldehyde (GTA) were prepared. Indeed, GTA-PVA gel is a well-known matrix able to mimic efficiently the physiological thermal properties of tissues [19]. The procedure used for the hydrogel preparation, described in detail elsewhere [20,21], is here briefly summarized. PVA-GTA hydrogel was prepared by mixing a PVA solution with a GTA solution. The PVA solution with final concentration of 8 % w/w was obtained by dissolving dry PVA (Mowiol®18-88, Sigma Aldrich) in 80% of the total ultrapure water used for the hydrogel preparation. Initially, the incorporation of PVA in water took place at 25°C under rapid stirring (~500 rpm) for about 5 minutes to avoid the formation of polymer aggregates. Next, the solution was heated up to 70 °C for 30 minutes with a progressive reduction of the stirring speed (~150 rpm). The GTA solution was prepared with 21.2 mM of glutaraldehyde (GTA, Sigma Aldrich), 20 mM of sulfuric acid (SA, Suprapur®, Sigma Aldrich) and the remaining 20% of the total water. PVA-GTA hydrogel was obtained by incorporating GTA solution into the PVA solution at 25°C.

PVA-GTA hydrogel was poured into cylindrical plastic containers (2.9 cm long and 2 cm in diameter) and bare fiducial markers were dispersed inside the hydrogel, at a depth of approximately 2 mm from the phantom surface. The position of the gold markers into the gels was chosen to test the possible influence of the geometrical arrangement. Two different configurations were considered. The first consisted in placing a single fiducial marker in the center of the hydrogel phantom. In this set-up the cylinder and the helical coil were inserted both vertically-oriented and horizontally-oriented with respect to the gel surface. In the second configuration, three cylinders were placed vertically at the vertices of an equilateral triangle of side equal to approximately 10 mm. It is worth noting that at least three fiducials markers must be implanted and visualized in IGRT procedures based on the real-time tracking of the tumor during the RT treatments, as in case of use of Cyberknife systems [22].

2.3 Magnetic stimulation and temperature measurement

The magnetic stimulation was obtained by means of Magnetherm (nanoThericsTM) set-up that builds up an AMF with amplitude values up to 17 kA/m, and a frequency range from 100 to 1000 kHz.

During the AMF stimulation of the carbon black covered fiducial markers a high-resolution thermal camera (FLIR A65 FLIR Systems Inc., 640x512 pixel, 0.05 K thermal resolution, 25 mm Germanium lens) was used to monitor the temperature variation of the fiducials over the time.

The same thermal camera was employed to monitor the temperature of the surface of the hydrogel phantoms containing the bare fiducials. Bare fiducials were used since the low emissivity of gold was overcome by measuring the temperature distribution over the neighboring hydrogel areas, being composed mostly by water, assuming an emissivity of 0.95 [18]. Furthermore, in case of phantoms, in addition to the surface-temperature mapping by the thermal camera, an optical fiber based sensor (Optocon^{TM}, Weidmann Technologies Deutschland GmbH, Germany, sensitivity 0.2°C), positioned at a depth of about 3 mm from the hydrogel surface, was used for point measurements of the temperature inside the hydrogel phantoms. In case of a single fiducial marker in the center of the hydrogel phantom, the sensor was placed at a distance of approximately 6 mm from the fiducial marker. When three fiducials are inserted into the hydrogel phantom, the sensor was in the center of the equilateral triangle, i.e. 6 mm far from each cylinder.

In order to mimic the thermal condition of the biological tissues subjected to a MFH treatment, an external custom-made thermalizer system based on a Lauda Alpha A (LAUDA-Brinkmann LP, New Jersey), thermostat circulating hot water around the sample was used to initially thermalize the hydrogel phantoms at 37°C. The AMF stimulation was therefore applied to the samples thermalized at 37°C. A picture of the instruments and a drawing of the experimental set-up are shown in Figure 2.

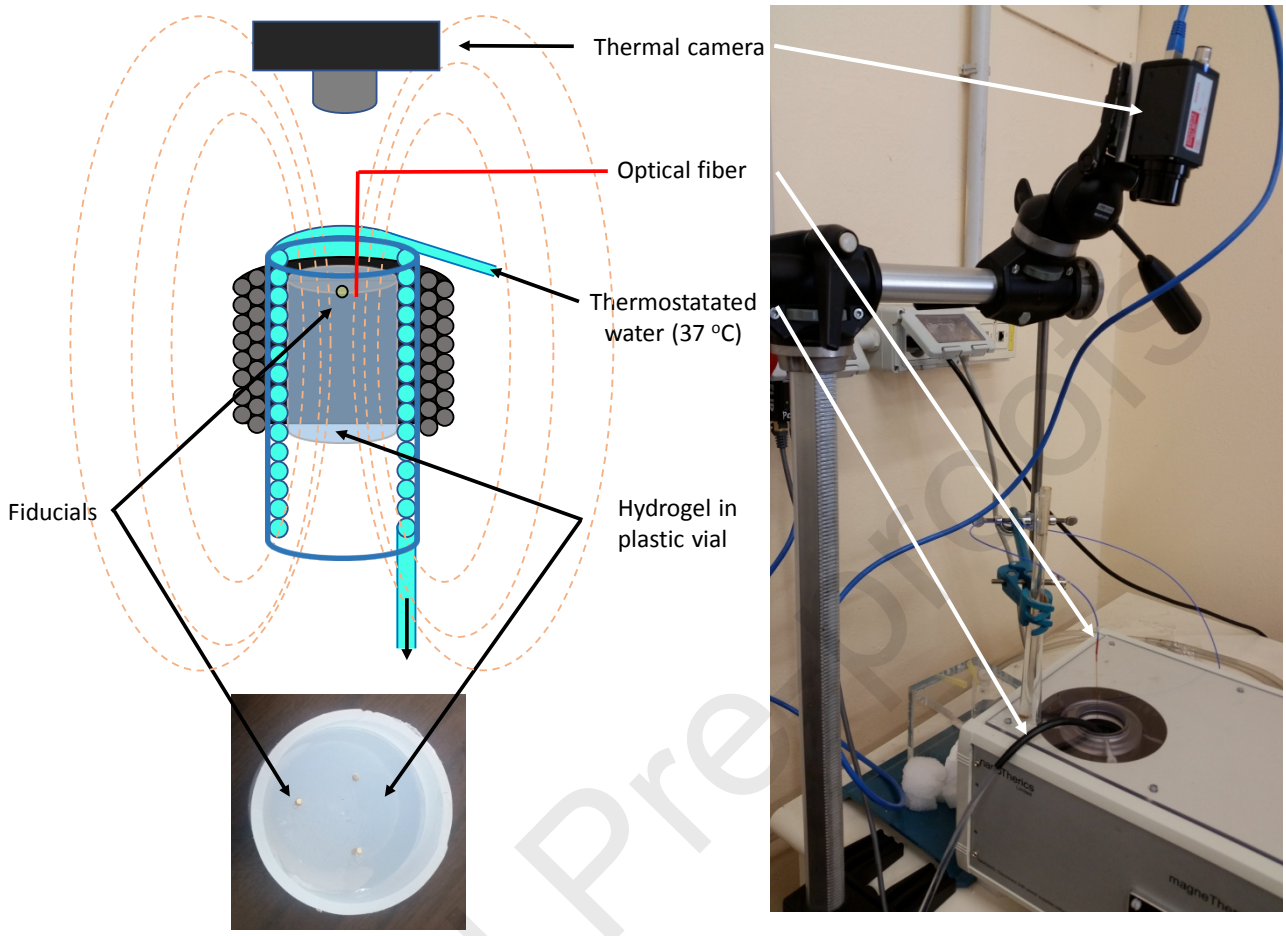

Figure 2. Sketch of the experimental set up used for measuring hyperthermia in hydrogel phantoms containing gold fiducial markers, by means of an alternating magnetic field (left). Picture of the experimental set up with indication of the main components required for the measurements (right).

3. Results and discussion

Figure 3 shows, as an example, the time-course profile of the temperature of the carbon black covered sphere without hydrogel phantom, during a thermal imaging analysis. After the start of the AMF stimulation, the temperature increased of more than 70°C in less than 30 seconds, reaching a final stable value of approximately 94°C. Similar trends were obtained with the cylinders, using the same experimental set-up.

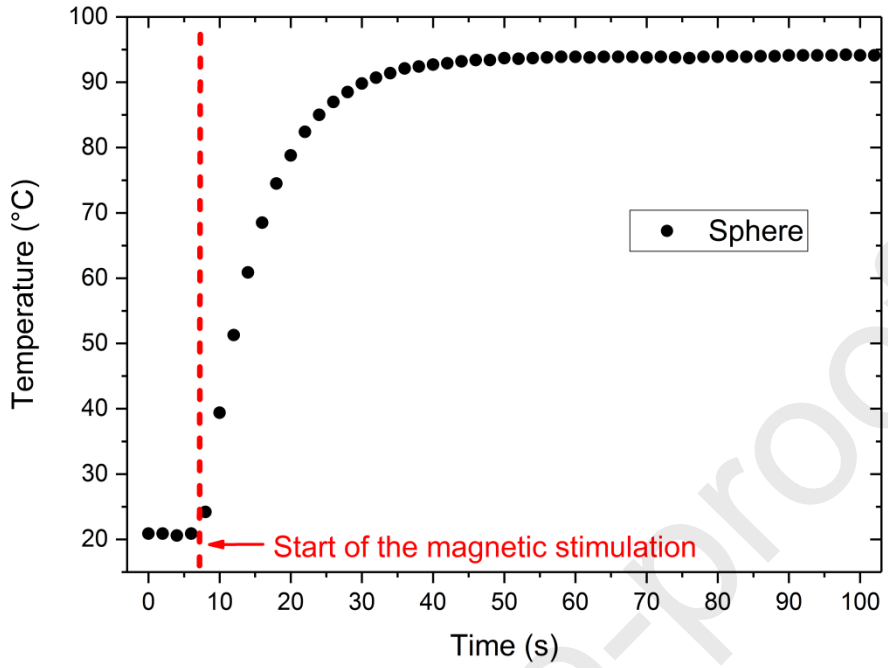

Figure 3. Temperature increase of the Bone Fiducial Marker (sphere, without hydrogel phantom) during the AMF stimulation. The error bars, corresponding to the resolution of 0.05 K of the thermal camera, are smaller than the symbols.

These results clearly demonstrated the possibility to induce the heating of the gold fiducial markers using a magnetic field with amplitude and frequency typically used in MFH procedures. The temperatures reached by the gold markers proved to be higher than those required to produce thermal ablation of biological systems, i.e. above 45-50°C [23,24].

Figure 4 shows the images of the hydrogel phantoms surface containing an individual sphere 2 mm deep in the hydrogel, acquired by the thermal camera 10, 30, 60, 120 and 240 seconds after the start of the AMF stimulation. The corresponding temperature profiles at different times, drawn along the white segment traced in Figure 4e, are shown in Figure 4f. These profiles were obtained considering the hydrogel only, i.e. avoiding the apparent cold spot of the fiducial marker due to the low emissivity of gold surface.

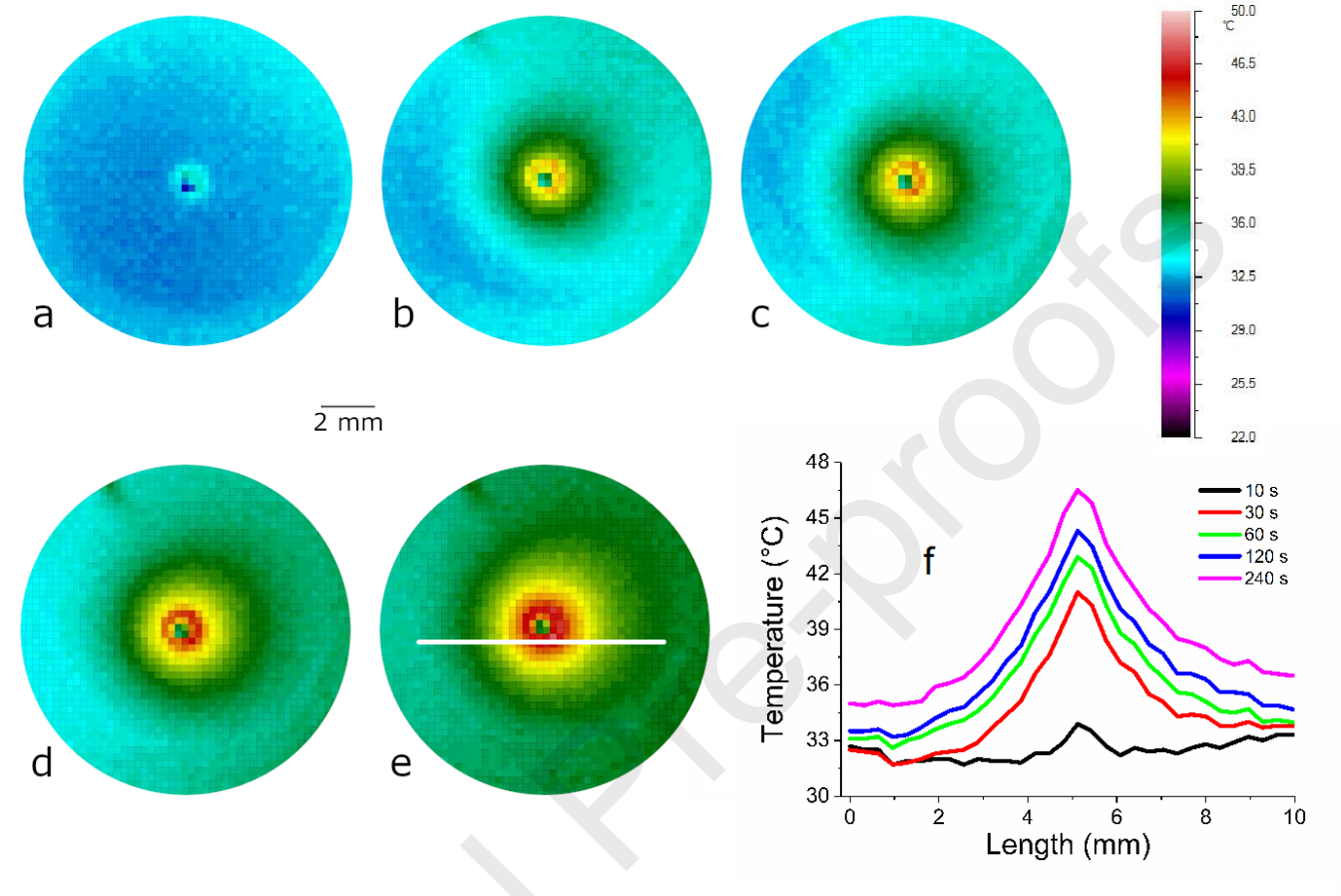

Figure 4. Thermal images of hydrogel surface with the Bone Fiducial Marker (sphere) at different times after the start of the AMF stimulation: a) 10 s, b) 30 s, c) 60 s, d) 120 s, e) 240 s. The apparent colder spot at the center of heated area is an effect of the low emissivity of the surface of gold. Figure 4f shows the temperature profiles drawn along the white segment traced in Figure 4e.

The thermal camera images of the hydrogel phantoms surface containing different individual fiducial markers acquired 60 seconds after the start of the AMF stimulation are shown in Figure 5. The heating curves measured by the optical fiber sensor, are given in Figure 6.

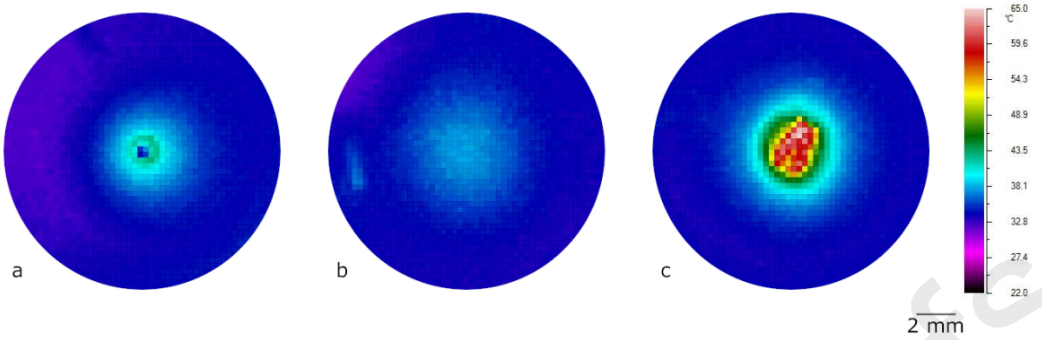

Figure 5. Thermal images of the hydrogel phantoms containing different individual fiducial markers acquired 60 seconds after the start of the AMF stimulation: a) Bone Fiducial Marker (sphere), b) PointCoil™ Fiducial Marker (vertically oriented helical coil), c) Gold Soft Tissue Marker (horizontally oriented cylinder). The images show different thermal range with respect to the one in Figure 4.

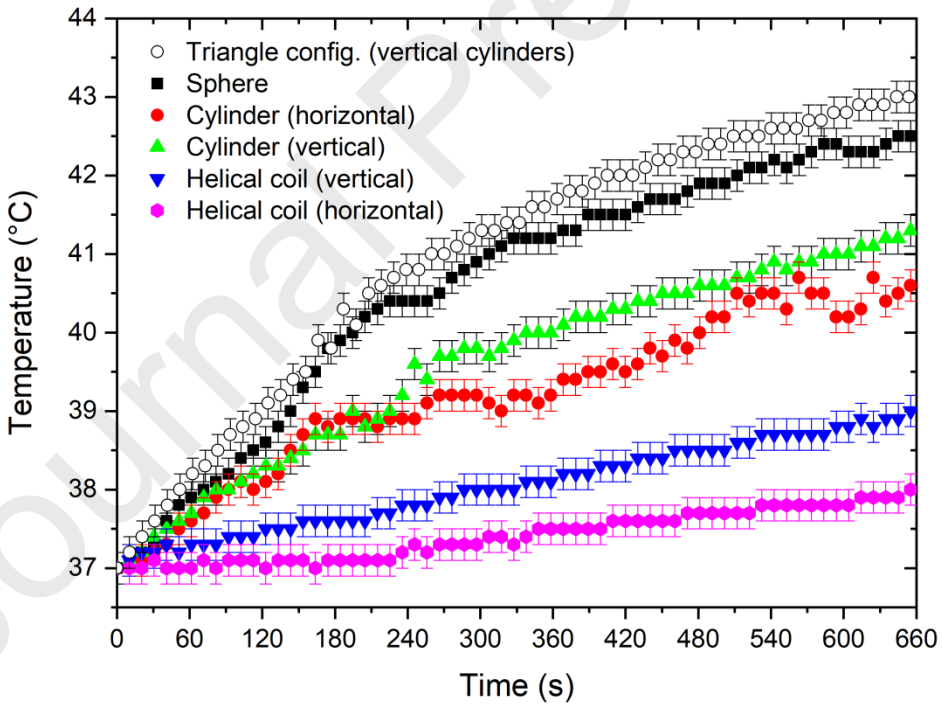

Figure 6. Heating curves inside the hydrogel phantom containing the different fiducial markers, measured by the optical fiber sensor. The error bars correspond to 0.2°C, according to the sensitivity of the instrument.

The thermal images, shown in Figure 5, revealed the progressive diffusion of the heat over the hydrogel surface, as effect of the increase of the temperature of the gold fiducial marker. The extent of such diffusion measured by the thermal camera depended on the type of fiducial marker and on the geometric configuration used. In particular, the diffusion was negligible in the case of the PointCoil™ Fiducial Marker regardless of the vertical or horizontal orientation.

The point measurements of the temperature inside the hydrogel phantom by the optical fibre sensor, shown in Figure 6, confirmed qualitatively the macroscopic results observed on the surface by the thermal camera. Indeed, the coil arrangement substantially caused a mild and slow warming in the hydrogel. On the other hand, the sphere and cylinder shapes presented a much faster temperature increase, especially in the first three minutes after the start of the AMF stimulation. The orientation of the cylinder seems to poorly affect the diffusion of heat in the hydrogel phantom. As expected, the simultaneous stimulation of more than one fiducial marker caused an enhancement of the hyperthermia effect, as proved by the heating curve measured in the triangle configuration. As showed in Figure 5 and 6 thermal camera and optical fiber sensor data present slight differences in temperature values. The reason is that thermography is a surface temperature measurement while the optical fiber measures the temperature inside a specific point of the hydrogel. In addition, different geometry of the fiducials cause non–homogeneity in the heat diffusion, as visualized by thermal camera.

Our results attested the increase of the temperature in the hydrogel phantoms as effect of the heating of the gold fiducial markers employed in IGRT procedures, when stimulated by an AMF in the typical instrumental conditions used at present in MFH clinical trials. Additionally, it makes sense to assume that the heat release by a fiducial marker in *in-vivo* condition should be higher. Indeed, in the performed measurements the upper side of the hydrogel was in contact with air implying a different heat exchange ways with respect to the “in body” situation, where the markers are surrounded by tissues at 37°C.

Therefore, in order to make one more step approaching to in-vivo condition, further studies will be performed by implementing larger hydrogel phantoms. For this experimental set up, in addition to the measurements of temperature distribution and heating curves inside the hydrogel phantom, the CEM 43°C index, extensively used as a threshold of thermal damage [25-28], will be also evaluated.

In MFH technique the energy release is due to the opening of the hysteresis loop that describe the evolution of the magnetization of superparamagnetic nanoparticles as a function of the oscillation of the AMF [29,30]. The nanoparticles magnetization, also called superspin, fluctuates naturally due to two relaxation mechanisms [31]: the Néel relaxation, i.e. the thermal reversal along an anisotropy-determined easy axis [32], and the Brown relaxation, i.e. the rotation of the nanoparticle, once dispersed in a solvent, due to the random collisions with the dispersant molecules [33]. An effective relaxation time τ can be defined to account for both the Néel and Brown relaxations, acting simultaneously [34]. When an AMF in a specific range of frequencies (that depends on τ) is applied, a dephasing between the particles' superspin and the external field occurs, causing the opening of the otherwise closed hysteresis loop and a transfer of energy from the field to the colloidal dispersion of nanoparticles, i.e. the heating [35,36]. Conversely, considering the bulk structure and dimensions of the investigated fiducial marker, as already said previously, it is reasonable to assume that the observed hyperthermia properties are due to the creation of eddy currents on their surfaces once excited by the AMF. In spite of the fact that further investigations are required in order to validate this hypothesis, it must be pointed out that ED-XRF measurements excluded the presence of any significant amount of other metal ions besides gold, thus the heat release cannot be correlated to hysteretic losses of an additive magnetic component. Moreover, to the best of our knowledge, at the typical frequencies used in MFH experiments, data proving thermal energy release by gold nanoparticles have not been reported in the literature to date.

4. Conclusions

In this study, the promising approach in oncology consisting in the combination of IGRT and MFH was considered. In particular, hyperthermia produced by different gold fiducial markers used for IGRT under the application of an alternating magnetic field in the typical conditions of MFH clinical trials was investigated. Measurements of the temperature increase of different types of gold fiducial markers and of tissue mimicking hydrogel phantoms containing the fiducials were performed during the magnetic stimulation using a high-resolution thermal camera and a fiber optic temperature sensor. Temperature values capable of thermal ablation in biological systems were revealed. Therefore, the experimental evidences of this study highlight the need to evaluate carefully the presence and location of gold fiducial markers in case of combined MFH and IGRT treatments, in order to prevent any pain and detriment for the patients. In fact, if the gold fiducial markers are not implanted into the tumor but in its proximity, an excessive heating during the MFH treatment might produce damages of the health tissues surrounding the markers.

Supplementary Material

See supplementary material for further details about Energy Dispersive X-Ray Fluorescence (ED-XRF) spectroscopy analyses performed on the fiducial markers.

Acknowledgments

This work was supported by the Department of Physics of the Università degli Studi di Milano. Authors are grateful to Dr.ssa Anna Galli of the CNR-IFN and Department of Materials Science of the Università degli Studi di Milano-Bicocca, Italy for her help in the ED-XRF analyses. Authors thank Dr. Antonio Lucarelli of Tema Sinergie for providing free samples of gold fiducial markers used in preliminary feasibility tests. P.A. thanks prof. Prof. Dr. Silvio Dutz of Technische Universität Ilmenau for the precious suggestions.

References

[1] D.A. Jaffray and M. K. Gospodarowicz, Disease Control Priorities – Third edition, Cancer, Editors H. Gelband, P. Jha, R. Sankaranarayanan, S. Horton, 2015 (International Bank for Reconstruction and Development / The World Bank, Washington, 2015) p. 239-247.

[2] J. De Los Santos, R. Popple, N. Agazaryan, J. E. Bayouth, J. P. Bissonnette, M. K Bucci, S Dieterich, L. Dong, K. M. Forster, D. Indelicato, K. Langen, J. Lehmann, N. Mayr, I. Parsai, W. Salter, M. Tomblyn, W.T.C. Yuh, I.J. Chetty, Image guided radiation therapy (IGRT) technologies for radiation therapy localization and delivery, Int J Radiation Oncol Biol Phys 87(1) (2013) 33-45.

[3] M.F. Chan, G.N. Cohen, J.O. Deasy, Qualitative evaluation of fiducial markers for radiotherapy imaging, Technology in Cancer Research & Treatment 14(3) (2015) 298-304.

[4] C.P. Nolan and E.J. Forde, A review of the use of fiducial markers for image-guided bladder radiotherapy, Acta Oncologica 55(5) (2016) 533-538.

[5] G. Maiorano, E. Mele, M. C. Frassanito, E. Restini, A. Athanassiouc, P. P. Pompa, Ultra-efficient, widely tunable gold nanoparticle-based fiducial markers for X-ray imaging, Nanoscale 8 (2016) 18921-18927.

[6] J. Beik, M. Jafariyan, A. Montazerabadi, A. Ghadimi-Daresajini, P.Tarighi, A. Mahmoudabadi, H. Ghaznavi, A. Shakeri-Zadeh, The benefits of folic acid-modified gold nanoparticles in CT-based molecular imaging: radiation dose reduction and image contrast enhancement, Artificial Cells, Nanomedicine, and Biotechnology 46(8) (2018) 1993-2001.

[7] M. Keshavarz,K. Moloudi, R. Paydar, Z. Abed, J. Beik, H. Ghaznavi, A. Shakeri-Zadeh, Alginate hydrogel co-loaded with cisplatin and gold nanoparticles for computed tomography image-guided chemotherapy, Journal of Biomaterials Applications 33(2) (2018) 161-169.

[8] S.V. Spirou, M.Basini, A. Lascialfari, C. Sangregorio, C. Innocenti, Magnetic Hyperthermia and Radiation Therapy: Radiobiological Principles and Current Practice, Nanomaterials 8 (2018) 401.

[9] K. Maier-Hauff, R. Rothe, R. Scholz, U. Gneveckow, P. Wust, B. Thiesen, A. Feussner, A. von Deimling, N. Waldoefner, R. Felix, A. Jordan, Intracranial Thermotherapy using Magnetic

Nanoparticles Combined with External Beam Radiotherapy: Results of a Feasibility Study on Patients with Glioblastoma MultiformeJ Neurooncol 81(1) (2007) 53-60.

[10] K. Maier-Hauff, F. Ulrich, D. Nestler, H. Niehoff, P. Wust, B. Thiesen, H. Orawa, V. Budach and A. Jordan, Efficacy and safety of intratumoral thermotherapy using magnetic iron-oxide nanoparticles combined with external beam radiotherapy on patients with recurrent glioblastoma multiforme, J Neurooncol 103 (2011) 317-324.

[11] J. Beik, M. Khateri, Z. Khosravi, S. K. Kamrava, S. Kooranifar, H. Ghaznavi, A. Shakeri-Zadeh, Gold nanoparticles in combinatorial cancer therapy strategies, Coordination Chemistry Reviews 387 (2019) 15 299-324.

[12] J. Beik, S. Khademi, N. Attaran, S. Sarkar, A. Shakeri-Zadeh, H. Ghaznavi, H. Ghadiri, A Nanotechnology-based Strategy to Increase the Efficiency of Cancer Diagnosis and Therapy: Folate-conjugated Gold Nanoparticles, Current Medicinal Chemistry, 24 (2017) 4399-4416.

[13] A. Neshastehriz, M. Tabei, S. Maleki, S. Eynali, A. Shakeri-Zadeh, Photothermal therapy using folate conjugated gold nanoparticles enhances the effects of 6MV X-ray on mouth epidermal carcinoma cells. Journal of Photochemistry and Photobiology B: Biology 172 (2017) 172:52-60.

[14] X. Huang, P. K. Jain, I. H. El-Sayed, M. A. El-Sayed, Plasmonic photothermal therapy (PPTT) using gold nanoparticles, Lasers in medical science 23(3) (2008) 217-228.

[15] N. S. Abadeer, C. J. Murphy, Recent progress in cancer thermal therapy using gold nanoparticles, The Journal of Physical Chemistry C 120(9) (2016) 4691-4716.

[16] MagForce AG, The Nanomedicine Company, https://www.magforce.com/en/home.html/ 2019 (accessed 15 February 2019).

[17] CIVCO Radiotherapy/Products/Fiducial Markers, https://civcort.com/ro/products/Fiducial-Markers.htm/ 2019 (accessed 15 February 2019).

[18] V. Bernard, E. Staffa, V. Mornstein, A. Bourek, Infrared camera assessment of skin surface temperature – Effect of emissivity, Physica Medica 29 (2013) 583-591.

[19] J. Coffel, E. Nuxoll, Poly(vinyl alcohol) tissue phantoms as a robust in vitro model for heat transfer, International Journal of Polymeric Materials and Polymeric Biomaterials 65(15) (2016) 797-806.

[20] S. Gallo, E. Artuso, M. G. Brambilla, G. Gambarini, C. Lenardi, A. F. Monti, A. Torresin, E. Pignoli, I. Veronese, Characterization of radiochromic PVA-GTA Fricke gels for dosimetry in X-rays external radiation therapy Journal of Physics D: Applied Physics 52(22) (2019) 225601.

[21] S. Gallo, G. Gambarini, I. Veronese, S. Argentiere, M. Gargano, L. Ianni, C. Lenardi, N. Ludwig, E. Pignoli, F. d'Errico, Does the gelation temperature or the sulfuric acid concentration influence the dosimetric properties of radiochromic PVA-GTA Xylenol Orange Fricke gels? Radiation Physics and Chemistry 160 (2019) 35-40.

[22] I Veronese, E. De Martin, A.S. Martinotti, M.L. Fumagalli, C. Vite, I. Redaelli, T. Malatesta, P. Mancosu, G. Beltramo, L. Fariselli, M.C. Cantone, Multi-institutional application of failure mode and effects analysis (FMEA) to CyberKnife stereotactic body radiation therapy (SBRT), Radiation Oncology 10 (2015) 132.

[23] J. P. McGahan and D. Gerald, Radiofrequency Ablation of the Liver: Current Status, American Journal of Roentgenology 176 (2001) 3.

[24] M. Friedman, I. Mikityansky, A. Kam, S.K. Libutti, M.M. Walther, Z. Neeman, J.K. Locklin, B.J. Wood, Radiofrequency Ablation of Cancer, Cardiovasc Intervent Radiol 27 (2004) 427-434.

[25] W. C. Dewey, L. E. Hopwood, S. A. Sapareto, L. E. Gerweck, Cellular responses to combinations of hyperthermia and radiation, Radiology 123 (2) (1977) 463-474.

[26] L. Roizin-Towle, J. P. Pirro, The response of human and rodent cells to yperthermia, International Journal of Radiation Oncology, Biology, Physics 20 (4) (1991) 751-756.

[27] J. Beik, Z. Abed, A. Ghadimi-Daresajini, M. Nourbakhsh, A. Shakeri-Zadeh, M. S.Ghasemi, M. B. Shiran, Measurements of nanoparticle-enhanced heating from 1 MHz ultrasound in solution and in mice bearing CT26 colon tumors, Journal of thermal biology 62 (2016) 84-89.

[28] J. Beik, M. B. Shiran, Z. Abed, I. Shiri, A. G. Daresajini, F. Farkhondeh, H. Ghaznavi, A. Shakeri-Zadeh, Gold nanoparticle-induced sonosensitization enhances the antitumor activity of ultrasound in colon tumor-bearing mice, Medical physics 45(9) (2018) 4306-4314.

[29] J. Carrey, B. Mehdaoui, M. Respaud, Simple models for dynamic hysteresis loop calculations of magnetic single-domain nanoparticles: Application to magnetic hyperthermia optimization, J. Appl. Phys., 109(8) (2011) 083921.

[30] D. Ortega, Q. A. Pankhurst, Magnetic hyperthermia, Nanoscience 1(60) (2013) 60-88.

[31] S. Laurent, S. Dutz, U.O. Häfeli, M. Mahmoudi, Magnetic fluid hyperthermia: focus on superparamagnetic iron oxide nanoparticles, Adv. Colloid Interface Sci. 166(1-2) (2011) 8-23.

[32] R. Hergt, S. Dutz, M. Zeisberger, Validity limits of the Néel relaxation model of magnetic nanoparticles for hyperthermia, Nanotechnology 21(1) (2010) 15706.

[33] B. Fischer, B. Huke, M. Lücke, R. Hempelmann, Brownian relaxation of magnetic colloids, J. Magn. Magn. Mater. 289 (2005) 74-77.

[34] R.E.Rosensweig, Heating magnetic fluid with alternating magnetic field, J. Magn. Magn. Mater. 252 (2002) 370-374.

[35] E.A. Périgo, G. Hemery, O. Sandre, D. Ortega, E. Garaio, F. Plazaola, F.J. Teran, Fundamentals and advances in magnetic hyperthermia, Appl. Phys. Rev. 2(4) (2015) 041302.

[36] Q.A. Pankhurst, N.K.T. Thanh, S.K. Jones, J. Dobson, Progress in applications of magnetic nanoparticles in biomedicine, J. Phys. D. Appl. Phys. 42(22) (2009) 224001.

UNIVERSITÀ DEGLI STUDI
DI MILANO
DIPARTIMENTO DI FISICA

Article title:
"Magnetic stimulation of gold fiducial markers used in Image-Guided Radiation Therapy: evidences of hyperthermia effects"

Authors: P. Arosio et al.,

Highlights

- In IGRT alternate magnetic field stimulates heating of Gold fiducial markers in MFH
- Temperature distribution mapping of fiducial markers in tissue-mimicking phantoms
- The temperature near the gold fiducial markers may induce thermal ablation
- Checking position of gold marker prevents health tissue damage in combined MFH/IGRT

Corresponding author:
Nicola Ludwig
Università degli Studi di Milano and INFN
via Giovanni Celoria 16 - 20133 Milano, ITALY
e-mail: nicola.ludwig@unimi.it